Degradation kinetics and mechanism of β-lactam antibiotics by the activation of H₂O₂ and Na₂S₂O₈ under UV-254 nm irradiation

Xuexiang He [a,c], Stephen P. Mezyk [b], Irene Michael [c],
Despo Fatta-Kassinos [c], Dionysios D. Dionysiou [a,c,*]

[a] Environmental Engineering and Science Program, University of Cincinnati, Cincinnati, OH 45221-0012, United States
[b] Department of Chemistry and Biochemistry, California State University Long Beach, 1250 Bellflower Blvd., Long Beach, CA 90840, United States
[c] Department of Civil and Environmental Engineering and Nireas-International Water Research Centre, School of Engineering, University of Cyprus, PO Box 20537, 1678 Nicosia, Cyprus

HIGHLIGHTS

- Removal efficiency was comparable at different UV fluence rates but same fluence.
- Reducing pH to 3 or 2 did not inhibit the removal of nitrobenzene by UV/S₂O₈²⁻.
- 1.84×10^{-14} M $[HO^\bullet]_{ss}$ and 3.10×10^{-13} M $[SO_4^{\bullet -}]_{ss}$ in UV/S₂O₈²⁻ were estimated.
- $HO^\bullet$ reacted faster with the β-lactams than $SO_4^{\bullet -}$ but sharing similar byproducts.
- Transformation pathways included hydroxylation, hydrolysis and decarboxylation.

GRAPHICAL ABSTRACT
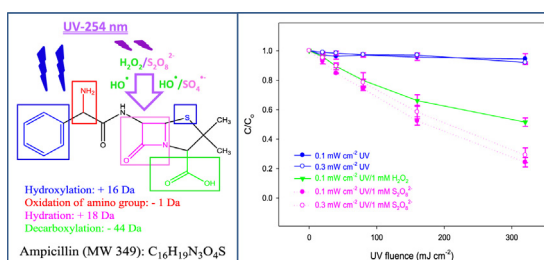
ARTICLE INFO

ABSTRACT

The extensive production and usage of antibiotics have led to an increasing occurrence of antibiotic residuals in various aquatic compartments, presenting a significant threat to both ecosystem and human health. This study investigated the degradation of selected β-lactam antibiotics (penicillins: ampicillin, penicillin V, and piperacillin; cephalosporin: cephalothin) by UV-254 nm activated H₂O₂ and S₂O₈²⁻ photochemical processes. The UV irradiation alone resulted in various degrees of direct photolysis of the antibiotics; while the addition of the oxidants improved significantly the removal efficiency. The steady-state radical concentrations were estimated, revealing a non-negligible contribution of hydroxyl radicals in the UV/S₂O₈²⁻ system. Mineralization of the β-lactams could be achieved at high UV fluence, with a slow formation of SO₄²⁻ and a much lower elimination of total organic carbon (TOC). The transformation mechanisms were also investigated showing the main reaction pathways of hydroxylation (+16 Da) at the aromatic ring and/or the sulfur atom, hydrolysis (+18 Da) at the β-lactam ring and decarboxylation (−44 Da) for the three penicillins. Oxidation of amine group was also observed for ampicillin. This study suggests that UV/H₂O₂ and UV/S₂O₈²⁻ advanced oxidation processes (AOPs) are capable of degrading β-lactam antibiotics decreasing consequently the antibiotic activity of treated waters.

© 2014 Elsevier B.V. All rights reserved.

* Corresponding author at: 705 Engineering Research Center, University of Cincinnati, Cincinnati, Ohio 45221-0012, United States. Tel.: +1 513 556 0724; fax: +1 513 556 4162.
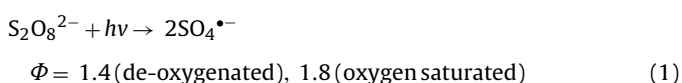E-mail addresses: dionysios.d.dionysiou@uc.edu, dionysdd@ucmail.uc.edu (D.D. Dionysiou).

1. Introduction

Antibiotics, one of the most widely used and frequently prescribed categories of pharmaceuticals, are applied not only for the inactivation or killing of microbes [1], but also for various animal husbandry and agricultural purposes [2]. The estimated annual use of antibiotics for human in Germany was 300 tons and for animals was 1700 t [3]. The annual consumption in the United States was estimated to be 3290 t for humans, 13,540 t for livestock, 150 t for aquaculture, 150 t for pets and 70 t for crops [2]. The Food and Drug Administration (FDA) reported that in 2011, more than 880 t of penicillin class of antibiotics and 26 t of cephalosporin class of antibiotics were approved for use in food-producing animals alone in the US [4]. Besides, up to 90% of human prescription antibiotic consumption can be excreted without undergoing metabolism [5]. The lack of an effective treatment before wastewater discharge can subsequently lead to their wide occurrence in natural environments [6–8]. The full impacts of the antibiotic residuals in the natural waters on the ecosystem and ultimately humans have yet to be fully evaluated [5,9]. Although acute toxicity may not be significant, a number of studies have gradually revealed the severe chronic toxicity of certain antibiotic species [10]. Their existence in the aquatic environment, even at very low concentration levels, can promote the growth of antibiotic resistant bacteria or pathogens [1,5,6,9–11].

A number of technologies have been developed for the removal of such microcontaminants in wastewater treatment plants [10]. Advanced oxidation processes (AOPs) are considered as promising alternatives to conventional wastewater treatment processes for water decontamination [10,12,13]. The main mechanism of AOPs is through the generation of highly reactive free radicals. Traditional AOPs mainly function by hydroxyl radicals (HO$^\bullet$, HR-AOPs) [14]; however, sulfate radical-based AOPs (SR-AOPs) have also been attracting significant scientific interest for the destruction of micropollutants such as pharmaceuticals and cyanotoxins [15–18].

The combination of UV-254 nm light, which has been extensively applied in water treatment facilities for disinfection purposes, with hydrogen peroxide, i.e., UV-254 nm/H$_2$O$_2$, is one of the most common ways to generate hydroxyl radicals [14]. UV/H$_2$O$_2$ has been demonstrated to be very effective in degrading various organic contaminants, including endocrine disrupting compounds, pharmaceuticals, pesticides, and cyanotoxins [14,16,18,19]. The single step dissociation of H$_2$O$_2$ to form hydroxyl radicals, with no sludge formation and potentially complete contaminant mineralization, has made it the most frequently applied oxidant in AOPs [20,21]. Persulfate (S$_2$O$_8{}^{2-}$, PS), on the other hand, has a high redox potential and is quite stable at room temperature. After activation, by UV, transition metals, and/or elevated temperature or pH, sulfate radicals (SO$_4{}^{\bullet-}$) can be generated [15]. Both UV/H$_2$O$_2$ and UV/PS processes could be influenced by natural water quality as suggested by the comparable reaction of HO$^\bullet$ and SO$_4{}^{\bullet-}$ at 8.5×10^6 and 9.1×10^6 M^{-1} s^{-1}, respectively, with natural alkalinity, i.e., HCO$_3{}^-$ [22,23]. Limited information is available on the reaction rate constant of natural organic matter (NOM) with SO$_4{}^{\bullet-}$. However, its reactivity is expected to be at least one order of magnitude lower than $k_{\text{HO}^\bullet/\text{NOM}}$ [24,25]. Besides, under UV-254 nm irradiation, S$_2$O$_8{}^{2-}$ has a much higher radical quantum yield than H$_2$O$_2$, as shown in Eqs. (1) and (2) [26,27]. In fact, a better performance of UV/PS than UV/H$_2$O$_2$ in the degradation of cyanotoxin cylindrospermopsin in various natural water samples has been reported [28].

$$S_2O_8{}^{2-} + h\nu \rightarrow 2SO_4{}^{\bullet-}$$

$$\Phi = 1.4 \,(\text{de-oxygenated}), \ 1.8 \,(\text{oxygen saturated}) \tag{1}$$

$$H_2O_2 + h\nu \rightarrow 2HO^\bullet \quad \Phi = 1.0 \tag{2}$$

The purpose of this study was to investigate the removal of selected β-lactam antibiotics (penicillins: ampicillin, penicillin V, and piperacillin; and cephalosporin: cephalothin) by UV-254 nm/H$_2$O$_2$ and UV-254 nm/S$_2$O$_8{}^{2-}$ AOPs. Since HO$^\bullet$ is non-selective and can react effectively through hydrogen atom abstraction (H-abstraction) and hydroxyl addition at the double bond [23], a modification of the β-lactam ring can thus be expected. On the other hand, SO$_4{}^{\bullet-}$ reaction occurs mainly by electron abstraction or to a lesser extent through H-abstraction [22]. Therefore, the elimination of a carboxylate, hydroxylation at the aromatic ring or the double bond of the β-lactams is more likely for sulfate radical reaction [29]. This study can thus provide valuable information on the elimination of the antibiotic reactivity by UV-AOPs through kinetic evaluation and transformation mechanism assessment. A high initial concentration of 50 μM of the pollutant was used in this study with the aim of quantitatively evaluating mineralization potential (e.g., in terms of sulfate anion formation and total organic carbon (TOC) elimination). The contribution of hydroxyl and sulfate radicals in UV/S$_2$O$_8{}^{2-}$ was examined. The reaction pathways were accessed through the identification of transformation products (TPs) by mass spectrometry.

## 2. Materials and methods

2.1. Materials

The antibiotics, ampicillin (AMP, sodium salt, Fisher), penicillin V (PEN, potassium salt, Fisher), piperacillin (PIP, sodium salt, Sigma Aldrich) and cephalothin (CEP, sodium salt, Sigma Aldrich), and the oxidants, H$_2$O$_2$ (50%, v:v, Fisher) and Na$_2$S$_2$O$_8$ (98%, Sigma Aldrich), as well as other chemicals were all ACS (American Chemical Society) grade and used as received. Table 1 shows the structure of the examined antibiotics.

2.2. Analysis

The concentration of organic compounds was determined by HPLC with a photodiode array detector. Three different methods were applied. Both methods no. 1 and 2 used an Agilent 1100 Series quaternary LC and a Nova-Pak C$_{18}$ Waters (3.9 × 150 mm, 5 μm) column with a mobile phase of 0.1% acetic acid in Milli-Q water (A) and 100% acetonitrile (B). Method no. 1 used an isocratic mode with 80% A and 20% B. Method no. 2 used a gradient analysis mode, starting with 95% A, and gradually changing to 65% A in 12 min, then back to 85% A in the next four minutes, and returning to 95% A in the last two minutes. Both methods had an identical injection volume of 20 μL, a flow rate of 0.5 mL min^{-1} and a column temperature of 25 °C. Method no. 3 used a C$_{18}$ Discovery HS (Supelco) column (2.1 × 150 mm, 5 μm) with a mobile phase of 0.05% (v/v) trifluoroacetic acid (TFA) in acetonitrile solution and 0.05% TFA in Milli-Q water in a 40:60 (v:v) ratio. A flow rate of 0.2 mL min^{-1}, an injection volume of 20 μL and a column temperature of 40 °C were applied. The competitors for determining second-order rate constant, i.e., para-chlorobenzoic acid (pCBA) and m-toluic acid (m-methylbenzoic acid, TA), were analyzed by either method no. 1 or 2 dependent on the other compound in the competing reaction solution. For example, at the determination of $k_{\text{HO}^\bullet/\text{AMP}}$, pCBA was analyzed by method no. 1; while at the determination of $k_{\text{HO}^\bullet/\text{CEP}}$, pCBA was analyzed by method no. 2. The limit of detection and quantification for each compound are listed in Table 2 [30].

The concentration of H$_2$O$_2$ and Na$_2$S$_2$O$_8$ was measured based on the spectrometric determination of triiodide complex at 352 nm resulting from the oxidation of iodide anion [31,32]. Sulfate anions were quantified by a Dionex Ion Chromatography equipped with

Table 1
Structures of model antibiotics.

Ampicillin ($C_{16}H_{18}N_3NaO_4S$, 371.4 g mol^{-1})
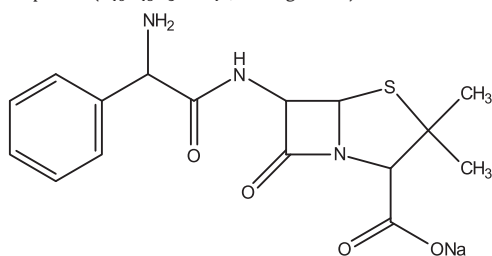
Penicillin V ($C_{16}H_{17}N_2O_5SK$, 388.5 g mol^{-1})
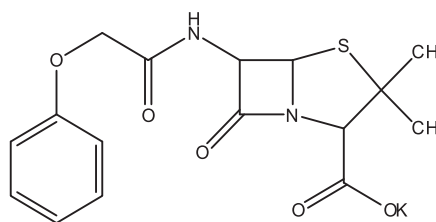
Piperacillin ($C_{23}H_{26}N_5NaO_7S$, 539.5 g mol^{-1})
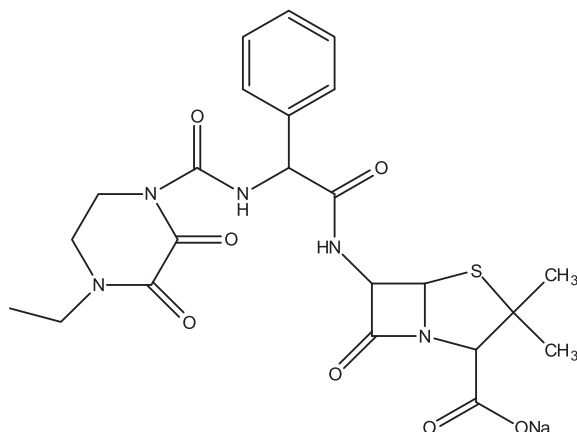
Cephalothin ($C_{16}H_{15}N_2NaO_6S_2$, 418.4 g mol^{-1})
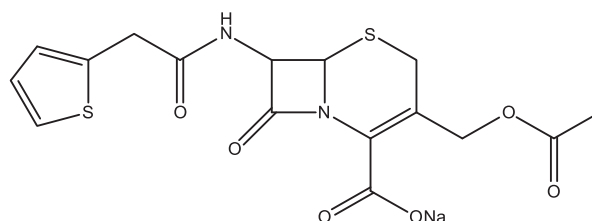
an IonPac® AS18 (2 × 250 mm) column and a guard column of IonPac® AG18 (2 × 50 mm). The eluent consisted of 3.5 mM Na_2CO_3 and 1.0 mM $NaHCO_3$. Sulfate anion was identified at a retention time of 6.6 min. TOC was measured as non-purgeable organic carbon by a Shimadzu VCSH-ASI TOC Analyzer. The analysis of the TPs generated during the processes was conducted using an Agilent 6540 ultra-high definition accurate-mass quadrupole time-of-flight (Q-TOF) liquid chromatography/mass spectrometer (LC-QTOF/MS). A sample volume of 10 μL was injected onto an Agilent ZORBAX Eclipse XDB-C18 narrow-bore rapid resolution column (2.1 × 50 mm, 3.5 μm). The mobile phase consisted of (A) 0.1% acetic acid in H_2O and (B) 0.1% acetic acid in methanol, with a gradient elution of 10% B linearly increased to 95% in the first seven min, and then back to 10% B in the next 0.1 min. Data were analyzed by Agilent MassHunter B.04.00 software.

2.3. Photolytic experiments

Experiments were carried out in a collimated beam system using two 15 W low-pressure UV lamps (Cole-Parmer) with monochromatic emission at $\lambda_{max} = 254$ nm. The average irradiance was determined to be 0.1 mW cm^{-2} [17]. The UV fluence (mJ cm^{-2}) used in this study was further calculated considering the absorbance of the water sample [33]. No buffer was used for pH control except where noted. The initial oxidant concentration of 1 mM and the initial antibiotic concentration of 50 μM were spiked in Milli-Q Water (Millipore Corp., Billerica, MA) if not stated otherwise. Samples were taken without adding any quenching agent and quickly injected into the HPLC for chemical quantification. For TP detection, samples were only taken at two UV fluence irradiation intervals, 40 and 640 mJ cm^{-2}. In this case, due to the sensitivity of the instrument, a lower initial antibiotic concentration of 25 μM in HPLC grade water (Sigma-Aldrich) was used.

In the competition studies for the determination of second-order rate constant, the initial concentrations of the antibiotics, pCBA, H_2O_2, and phosphate buffer (pH = 7.4) were 50 μM, 50 μM, 10 mM, and 5 mM, respectively, for $k_{HO^\bullet}$ determination; while those of the antibiotics, TA, $Na_2S_2O_8$, t-BuOH and phosphate buffer (pH = 7.4) were 50 μM, 50 μM, 10 mM, 500 mM and 5 mM,

Table 2
A summary on the analysis of organic compounds.

| Compound name (abbreviation)	Method no.	Detection wavelength (nm)	Retention time (min)	Limit of detection ($\times 10^{-7}$ M)	Limit of quantification ($\times 10^{-6}$ M)
Ampicillin (AMP)	1	238	5.9	3.65	1.29
Penicillin (PEN)	1	238	2.9	9.08	3.22
Piperacillin (PIP)	2	254	8.6	1.63	0.579
Cephalothin (CEP)	2	238	5.1	2.26	0.802
Nitrobenzene (NB)	1	254	3.2	3.08	1.09
para-Nitrobenzoic Acid (pNBA)	3	254	4.1	0.196	0.0694
para-Chlorobenzoic Acid (pCBA)	1	238	3.1	0.235	0.0931
	2	254	5.2	1.99	0.704
Benzoic acid (BA)	3	238	3.5	0.189	0.0671
m-Toluic acid (TA)	1	238	3.0	2.04	0.722
	2	238	4.3	2.46	0.871
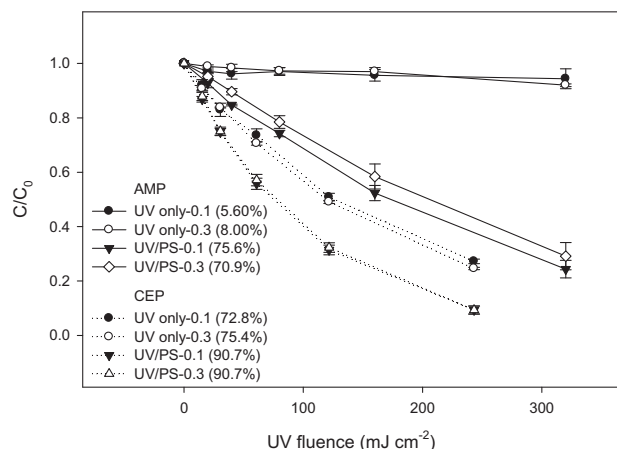
Fig. 1. Degradation of AMP and CEP by direct UV photolysis and UV/PS AOP. (a) $[AMP]_0 = 50 \mu M$, $[PS]_0 = 0$ or 1 mM; (b) $[CEP]_0 = 50 \mu M$; $[PS]_0 = 0$ or 1 mM. The numbers "0.1" and "0.3" represent the experiments were conducted at a UV fluence rate of 0.1 mW cm^{-2} and 0.3 mW cm^{-2}, respectively. The numbers in parenthesis are the percentage degradation rate at 320 mJ cm^{-2} for AMP and 240 mJ cm^{-2} for CEP, respectively.

Fig. 2. Degradation of nitrobenzene (NB) at various conditions. $[NB]_0 = 50 \mu M$; pH = 7.4 was prepared by 5 mM phosphate buffer; and pH 2 and 3 were adjusted using sulfuric acid.

respectively, for $k_{SO_4^{\bullet -}}$ determination. The UV direct photolysis was also considered in the rate constant calculation.

3. Results and discussion

3.1. Influence of UV fluence rate

Beside its germicidal purposes, UV-254 nm irradiation is capable of destroying a large variety of organic pollutants by direct photon absorption that excites molecules to high electronic states which can subsequently lead to bond cleavage [20,34]. Organic compounds with higher molar absorptivity at 254 nm thus have a higher potential for direct photolytic degradation. On the other hand, indirect degradation also occurs through the generation of reactive radicals due to the absorption of UV photons by an added oxidant, as shown in Eqs. (1) and (2) [26,27]. The degradation kinetics are thus highly correlated with the UV photons delivered.

The molar absorption coefficient at 254 nm, ε_{254} (M^{-1} cm^{-1}), was calculated according to Beer–Lambert law, $\varepsilon_{254} = A/c\,l$, where A is the measured absorbance, c is the concentration of the chemical to be analyzed (mol L^{-1}), and l is the path length (1.00 cm in this study). The ε_{254} of AMP was determined to be 300 M^{-1} cm^{-1}, and that of CEP to be 9200 M^{-1} cm^{-1} at 254 nm. This significant difference probably contributed to the faster direct photolysis of CEP than AMP as shown in Fig. 1 [34–36]. Considering the minimal destruction by persulfate under the dark reaction condition (i.e., 4.00% degradation of AMP at 985 min and 1.08% degradation of CEP at 54 min corresponding to 240 mJ cm^{-2} equivalence, data not shown), the increased degradation of the two antibiotics by UV/PS was probably attributed to the generated radical species [26]. The two different UV fluence rates, i.e., 0.1 and 0.3 mW cm^{-2}, resulted in comparable degradation of the target compounds at the same UV fluence. In other words, though at different UV fluence rates, so long as the UV photons entering the reaction solution are kept the same (as represented by UV fluence (mJ cm^{-2}), which equals to UV fluence rate (mW cm^{-2}) × time (s)), the same or comparable degradation of the target compound can be observed. Consequently, the following results interpretation and discussion will mainly focus on the use of UV flux instead of irradiation time except stated otherwise [35].
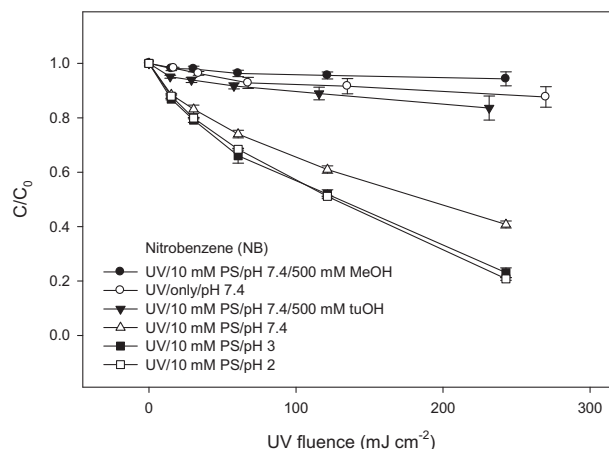
3.2. Qualitative contribution of hydroxyl radical in the UV/PS system

In the UV/PS system, both the sulfate radical and hydroxyl radical can be present as shown in Eq. (3) [37]. When there was no pH control, the decreased pH by the UV irradiation of persulfate during the reaction might lead to less transformation of SO$_4^{\bullet -}$ into HO$^{\bullet}$, suggesting the predominant existence of sulfate radical in the UV/PS system at lower pH conditions.

$$SO_4^{\bullet -} + OH^- \rightarrow SO_4^{2-} + HO^{\bullet} \quad k = 7 \times 10^7 \, M^{-1} \, s^{-1} \quad (3)$$
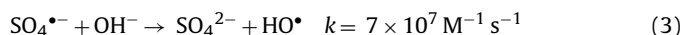
To ascertain the extent of hydroxyl radical contribution in the UV/PS system, nitrobenzene (NB), which barely reacts with sulfate radical as suggested by its second-order rate constants of <10^6 M^{-1} s^{-1} with sulfate radical [38] and 3.9×10^9 M^{-1} s^{-1} with hydroxyl radical [23], was used as a probe. As shown in Fig. 2, there was no significant degradation of NB by UV-only condition; while the presence of PS improved the removal efficiency. Reducing pH to 2–3 (i.e., $[OH^-] = 10^{-12}$–10^{-11} M) by adding an appropriate amount of sulfuric acid, however, did not slow down this degradation. The presence of a much higher concentration (500 mM) of either methanol (MeOH, $k_{HO^{\bullet}/MeOH} = 9.7 \times 10^8$ M^{-1} s^{-1}, [23]; $k_{SO_4^{\bullet -}/MeOH} = 1 \times 10^7 M^{-1} s^{-1}$, [39]) or tert-butanol (t-BuOH, $k_{HO^{\bullet}/t-BuOH} = 6.0 \times 10^8$ M^{-1} s^{-1}, [23]; $k_{SO_4^{\bullet -}/t-BuOH} = 8.4 \times 10^5 M^{-1} s^{-1}$, [39]) inhibited strongly the degradation of NB. The hydroxyl radical was, therefore, implicated in the UV/PS treatment process at pH 7.4. The t-BuOH was further chosen as a hydroxyl radical quenching agent for the determination of second-order rate constants between the organic compounds and sulfate radicals in this study [17,40,41]. Nevertheless, when MeOH was used as a quenching agent, a comparable rate constant for PIP and the sulfate radical could be obtained, i.e., 1.80 and 1.85×10^9 M^{-1} s^{-1}, in the presence of MeOH (this study) and previously reported t-BuOH [42], respectively.

3.3. Influence of H2O2 and certain inorganic anions

In UV-AOPs, beside the direct UV photolysis of the organic compound and the photolytic dissociation of the oxidant for radical generation, a major efficiency influencing factor is the reaction of the target compound with the radical species. Through competition kinetics measurements, the second-order rate constants of model

Table 3
Second-order rate constant (previously reported and currently determined) and the observed UV fluence based *pseudo first-order* rate constant at various reaction conditions. [Organic compound]$_0$ = 50 μM.

	k_{obs} ($\times 10^{-3}$ cm^2 mJ^{-1})			k ($\times 10^9$ M^{-1} s^{-1})		Percentage contribution in UV/S$_2$O$_8^{2-}$		
	UV only	UV/H$_2$O$_2$	UV/S$_2$O$_8^{2-}$	HO$^\bullet$	SO$_4^{\bullet-}$	UV	HO$^\bullet$	SO$_4^{\bullet-}$
AMP	0.24[a]	2.10 ± 0.15[a]	4.23 ± 0.36[a]	4.87[b]	2.00[b]			
CEP	5.56 ± 0.10[a]	7.79 ± 0.0.39[a]	9.87 ± 0.43[a]	5.37[b]	3.48[b]			
PEN	1.37 ± 0.19[a]	2.90[a]	3.18 ± 0.28[a]	6.54[b]	2.39[b]			
PIP	0.18[a,c]	1.46 ± 0.36[a,c]	3.81 ± 0.14[a,c]	8.21[c]	1.85[c]			
NB	0.306 ± 0.24	1.89 ± 0.29	0.954 ± 0.15	3.9[d]	<10^{-3}[e]	29.8%	69.9%	0.30%
pNBA	–	1.25	0.526	2.6[d]	<10^{-3}[e]	–	99.4%	0.64%
pCBA	0.157 ± 0.06	3.64 ± 0.32	2.31 ± 0.33	4.5[d]	0.36[e]	7.47%	39.4%	53.1%
BA	0.02 + 0.00	3.18 ± 0.20	3.11 ± 0.69	4.3[d]	1.2[e]	0.44%	17.5%	82.1%
TA	–	3.76 ± 0.06	8.88 ± 0.90	8[f]	2.0[e]	–	19.2%	80.8%

Note: [a] without pH control; while all the other experiments presented in this table were carried out at pH 7.4 as adjusted by 5 mM phosphate buffer; [b] determined in this study; [c] Mezyk et al. [42]; [d] Buxton et al. [23]; [e] Neta et al. [38]; [f] this value is in fact the rate constant of *p*-methylbenzoic acid with hydroxyl radical at pH 9. There is no value for TA as far as we know.

antibiotics with hydroxyl and sulfate radical were determined, as shown in Table 3. It was found that the reaction of model antibiotics with the sulfate radical was generally slower than that with hydroxyl radical. Hence the faster degradation efficiency of either AMP or CEP by UV/PS than by UV/H$_2$O$_2$ (as shown in Figs. 1 and 3) was probably resulted from the higher radical quantum yield (Eq. (1) vs (2)) of S$_2$O$_8^{2-}$ under UV irradiation. H$_2$O$_2$ has sometimes been combined with persulfate for a potential synergistic effect, which is, however, highly dependent on the reaction conditions such as the ratio of the oxidants, oxidant concentrations and pH [43]. With the experimental conditions applied in current study, no synergistic effect was observed. Moreover, both hydroxyl and sulfate radical can react with Cl$^-$ to form Cl$^\bullet$, which subsequently transforms into Cl$_2^{\bullet-}$, as shown in Eqs. (4)–(8) [22,44,45]. Considering the high Cl$^-$ concentration of 5 mM vs 50 μM of the parent compound, the quenching of HO$^\bullet$ and SO$_4^{\bullet-}$ may lead to an inhibition in the degradation of the antibiotics in the presence of Cl$^-$. However, only a slight impact of Cl$^-$ on the degradation of AMP or CEP by UV/PS was observed in this study (Fig. 3). A plausible explanation can be derived from the selective reaction of the chlorine radical species with the electron rich antibiotics [16,46,47]. The presence of other inorganic anions such as nitrate and sulfate at the 5 mM level did not affect the degradation efficiency either [46].
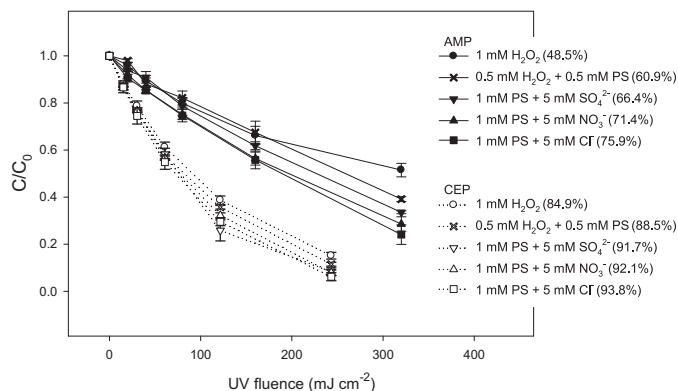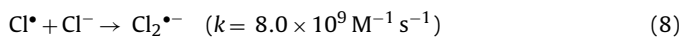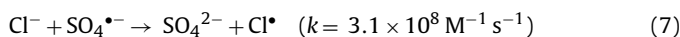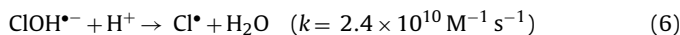
$$Cl^- + {}^\bullet OH \rightarrow ClOH^{\bullet-} \quad (k = 4.2 \times 10^9 \, M^{-1} \, s^{-1}) \quad (4)$$

$$ClOH^{\bullet-} \rightarrow Cl^- + {}^\bullet OH \quad (k = 6.0 \times 10^9 \, M^{-1} \, s^{-1}) \quad (5)$$

$$ClOH^{\bullet-} + H^+ \rightarrow Cl^\bullet + H_2O \quad (k = 2.4 \times 10^{10} \, M^{-1} \, s^{-1}) \quad (6)$$

$$Cl^- + SO_4^{\bullet-} \rightarrow SO_4^{2-} + Cl^\bullet \quad (k = 3.1 \times 10^8 \, M^{-1} \, s^{-1}) \quad (7)$$

$$Cl^\bullet + Cl^- \rightarrow Cl_2^{\bullet-} \quad (k = 8.0 \times 10^9 \, M^{-1} \, s^{-1}) \quad (8)$$
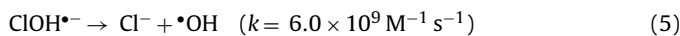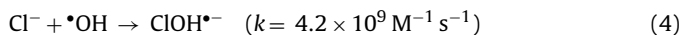

Fig. 3. The influence of H$_2$O$_2$ and certain inorganic anion for UV/PS. [AMP]$_0$ = 50 μM; [CEP]$_0$ = 50 μM. The numbers in parenthesis are the percentage degradation at 320 mJ cm^{-2} for AMP and 240 mJ cm^{-2} for CEP, respectively.

3.4. Quantification of hydroxyl and sulfate radical in the UV/H$_2$O$_2$ and UV/PS systems

Due to the selective reactivity of the sulfate radical, the degradation of certain organic compounds, such as nitrobenzene (NB), para-nitrobenzoic acid (pNBA) and para-chlorobenzoic acid (pCBA) can be even slower in the UV/PS than in the UV/H$_2$O$_2$ system, as suggested by their reported second-order rate constants [23,38] and currently determined UV fluence-based *pseudo first-order* rate constants, as shown in Table 3. As discussed above, the hydroxyl radical was the main reacting radical species in the UV/H$_2$O$_2$ AOP, while both hydroxyl and sulfate radical could result in the destruction of organic pollutants in the UV/PS AOP. To further identify the contribution of hydroxyl radical in the UV/PS system, a series of experiments was carried out for the quantification of these two radical species. Five compounds, i.e., NB, pNBA, pCBA, benzoic acid (BA) and TA, were used as model compounds for this process.

The concentrations of the oxidants did not change significantly under the conditions applied; hence steady-state radical concentrations could be assumed [48]. According to Eq. (9), the degradation rate of NB ($-d[NB]/dt$) in the UV/H$_2$O$_2$ system was directly correlated with the second-order rate constant of this compound with hydroxyl radical ($k_{HO^\bullet/NB}$), steady state radical concentration ([HO$^\bullet$]$_{ss}$), and the concentration of the target compound ([NB]). Eqs. (10)–(13) were then obtained by applying the currently determined UV fluence-based degradation rate constant (k_{obs}). The average [HO$^\bullet$]$_{ss,UV/H_2O_2}$ was then calculated using these five probe compounds.

$$-\frac{d[NB]}{dt} = k_{HO^\bullet/NB}[HO^\bullet]_{ss}[NB] \quad (9)$$

$$-\ln\frac{[NB]}{[NB]_o} = kt \quad (10)$$

where

$$\begin{aligned} k(s^{-1}) &= k_{HO^\bullet/NB}(M^{-1} \, s^{-1})[HO^\bullet]_{ss}(M) \\ &= k_{obs,HO^\bullet/NB}(cm^2 \, mJ^{-1}) \times 0.1 \, mW \, cm^{-2} \end{aligned} \quad (11)$$

$$[HO^\bullet]_{ss,UV/H_2O_2} = \frac{0.1 mW \, cm^{-2} k_{obs,HO^\bullet/NB}}{k_{HO^\bullet/NB}} \quad (12)$$

where

$$k_{obs,HO^\bullet/NB} = k_{obs,UV/H_2O_2/NB} - k_{obs,UV only/NB} \quad (13)$$

The second-order rate constants of NB and pNBA with the sulfate radical were reported to be three orders of magnitude lower than those with hydroxyl radical [23,38]. They were therefore chosen as probes to quantify the hydroxyl radical in the UV/PS

system. Assuming $5\% \times [SO_4^{\bullet-}]_{ss} < [HO^{\bullet}]_{ss} < 100\% \times [SO_4^{\bullet-}]_{ss}$ in the UV/PS system, Eqs. (14)–(16) could then be obtained. The average hydroxyl radical concentration determined using NB and pNBA, $[HO^{\bullet}]_{ss,UV/PS,average}$, was subsequently used to calculate the concentration of sulfate radical at steady-state using other probe compounds such as TA which has a rate constant at $10^9\,M^{-1}\,s^{-1}$ with both hydroxyl radical and sulfate radical (Eqs. (17) and (18), Table 3).

$$k_{obs,HO^{\bullet}/NB} = k_{obs,UV/PS/NB} - k_{obs,UV\,only/NB} - k_{obs,SO_4^{\bullet-}/NB} \qquad (14)$$

$$k_{HO^{\bullet}/NB}[HO^{\bullet}]_{ss}/(0.1\,mW\,cm^{-2})$$
$$= k_{obs,UV/PS/NB} - k_{obs,UV\,only/NB} - k_{SO_4^{\bullet-}/NB}[SO_4^{\bullet-}]_{ss}/(0.1\,mW\,cm^{-2})$$
$$\approx k_{obs,UV/PS/NB} - k_{obs,UV\,only/NB} \qquad (15)$$

$$[HO^{\bullet}]_{ss,UV/PS} = \frac{0.1mW\,cm^{-2}\left(k_{obs,UV/PS/NB} - k_{obs,UV\,only/NB}\right)}{k_{HO^{\bullet}/NB}} \qquad (16)$$

$$k_{obs,SO_4^{\bullet-}/TA} = k_{obs,UV/PS/TA} - k_{obs,UV\,only/TA}$$
$$- k_{HO^{\bullet}/TA}[HO^{\bullet}]_{ss,UV/PS,average}/10\,mW\,cm^{-2} \qquad (17)$$

$$[SO_4^{\bullet-}]_{ss,UV/PS} = \frac{0.1mW\,cm^{-2}k_{obs,SO_4^{\bullet-}/TA}}{k_{SO_4^{\bullet-}/TA}} \qquad (18)$$

The average radical concentrations were consequently estimated under $0.1\,mW\,cm^{-2}$ UV irradiation, 5 mM phosphate buffer (pH = 7.4), 1 mM initial oxidant and 50 μM initial organic compound conditions to be $5.73 \pm 0.75 \times 10^{-14}\,M$ $[HO^{\bullet}]_{ss}$ (mean ± standard error) in UV/H$_2$O$_2$, and $1.84 \pm 0.18 \times 10^{-14}\,M$ $[HO^{\bullet}]_{ss}$ and $3.10 \pm 0.59 \times 10^{-13}\,M$ $[SO_4^{\bullet-}]_{ss}$ in UV/PS. The results met the above mentioned assumption, i.e., $5\% \times [SO_4^{\bullet-}]_{ss} < [HO^{\bullet}]_{ss} < 100\% \times [SO_4^{\bullet-}]_{ss}$. The percentage contribution of the UV photolyis, HO$^{\bullet}$ reaction and SO$_4^{\bullet-}$ reaction was then calculated, revealing again the non-negligible contribution of HO$^{\bullet}$ in the UV/PS system, as shown in Table 3. Especially for compounds with a lower reaction rate constant with sulfate radical, such as NB and pNBA, HO$^{\bullet}$ was mainly responsible for their degradation in UV/PS at the conditions applied in this study.

3.5. Mineralization in terms of TOC elimination and SO$_4^{2-}$ formation

There was no interference of persulfate on SO$_4^{2-}$ analysis by IC; however, SO$_4^{2-}$ generation from the photolysis of persulfate had a significant influence on the measurement of SO$_4^{2-}$ released from the antibiotics. Hence the mineralization in terms of SO$_4^{2-}$ formation in this study was only evaluated for the UV/H$_2$O$_2$ process. The UV–vis absorption of the water solution changed significantly during the experimental period, the correction of UV fluence was thus not performed and the reaction time was used directly to make the plots. As seen in Fig. 4, although there was strong degradation of the parent compound at 54 min (i.e., $320\,mJ\,cm^{-2}$ for AMP and $240\,mJ\,cm^{-2}$ for CEP in Fig. 1), the release of sulfur as SO$_4^{2-}$ was much slower. The SO$_4^{2-}$ formed linearly by increasing UV photons entering into the reaction solution, with a linear regression rate of 1.56×10^{-2} (R^2 = 0.98) and 6.22×10^{-3} (R^2 = 0.96) mg L^{-1} min^{-1}, and a sulfur release of 94.8% and 75.2% at 588 min, respectively, for CEP and AMP. While the main purpose of AOPs is to destroy target pollutants, a complete mineralization was less favored with a low UV fluence. In fact, a good TOC removal was barely achieved even with 588 min UV irradiation, at 15.3% and 13.9% in UV/H$_2$O$_2$; 25.5% and 33.0% in UV/PS, respectively, for CEP and AMP. In a previous study on the degradation of 18.6 μM atrazine, only 62.9% and 44.1%

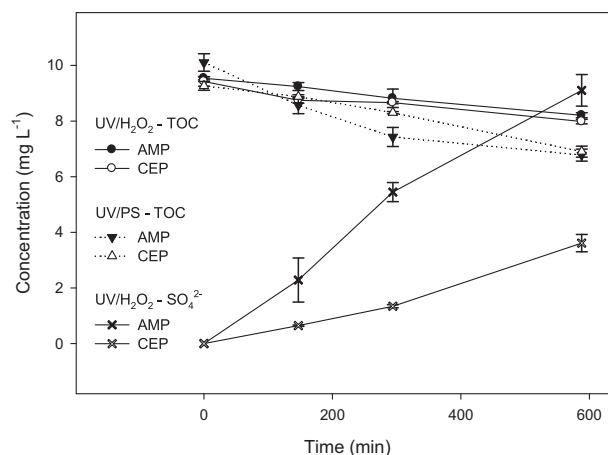**Fig. 4.** Mineralization in terms of TOC elimination (in both UV/H$_2$O$_2$ and UV/PS AOPs) and SO$_4^{2-}$ formation (in the UV/H$_2$O$_2$ AOP). [Antibiotics]$_0$ = 50 μM; [oxidant]$_0$ = 1 mM.

removal of TOC was reported at UV fluence as high as $6000\,mJ\,cm^{-2}$ with an initial Fe^{2+} concentration of 17.9 μM, and 1.86 mM PS and H$_2$O$_2$, respectively at pH = 3 [18]. Nevertheless, a complete mineralization of organic pollutants can still be achieved by optimizing the operational conditions such as by increasing reaction temperature or the oxidant dose [49,50]. UV/PS was shown to be slightly better than UV/H$_2$O$_2$ in TOC removal in this study, which was consistent with above discussion on its higher degradation efficiency of parent antibiotics. Comparable mineralization results were also obtained for the other two antibiotics, i.e., PEN and PIP, with 4.65 (R^2 = 0.99) and 4.52×10^{-3} (R^2 = 1.00) mg L^{-1} min^{-1} linear regression rate of sulfate formation, 58.5% and 55.5% sulfur release, and TOC removal of 11.6% and 3.20% in UV/H$_2$O$_2$, as well as 17.0% and 14.7% TOC removal in UV/PS, respectively.

3.6. Reaction pathways

3.6.1. AMP in the UV/H$_2$O$_2$ and UV/PS systems

There was no significant direct photolysis of AMP by the UV irradiation alone process; the degradation of AMP was therefore resulted only from radical reaction, i.e., hydroxyl radical, in UV/H$_2$O$_2$. There are four significant groups of TPs formed by hydroxyl radical reaction with AMP, through hydroxylation (+16 Da), hydrolysis (+18 Da), decarboxylation (−44 Da) and oxidation of amine into a carbonyl (−1 Da) (Fig. 5). The following observations were made:

(1) The aromatic ring was proposed to be the predominant hydroxylation reaction site for hydroxyl radical reaction with β-lactam antibiotics [51]. In this study, four different isomers were observed for +16 Da TPs P$_{366}$ (m/z 366, C$_{16}$H$_{19}$N$_3$O$_5$S), as shown in the extracted ion chromatogram (EIC), indicating a potential second reaction site at the sulfur atom. In fact, the reaction of sulfide (thioether) with HO$^{\bullet}$ through electron abstraction is very fast, leading to the formation a >S$^{\bullet}$—OH adduct [52]. The large substituent at the lactam ring probably inhibits the formation of a dimer radical cation [40]. The simple radical cation >S$^{\bullet+}$ and its subsequent oxidation TPs >S═O could thus be formed. (2) The +18 Da TPs P$_{368}$ (C$_{16}$H$_{21}$N$_3$O$_5$S) were at a significant abundance for both data points analyzed. As a comparison, 25 μM AMP standard solution was placed in dark at room temperature and analyzed after 20 h; the P$_{368}$ was also detected but at a much smaller abundance. This showed that the hydrolysis of the antibiotics was strongly promoted by the AOPs [53]. The opening of the β-lactam ring could then lead to the decrease in the antibiotic activity. (3) Electron abstraction from the carboxylate with the subsequent release of a CO$_2$ is known for hydroxyl radical reaction [29,54–56]. Through
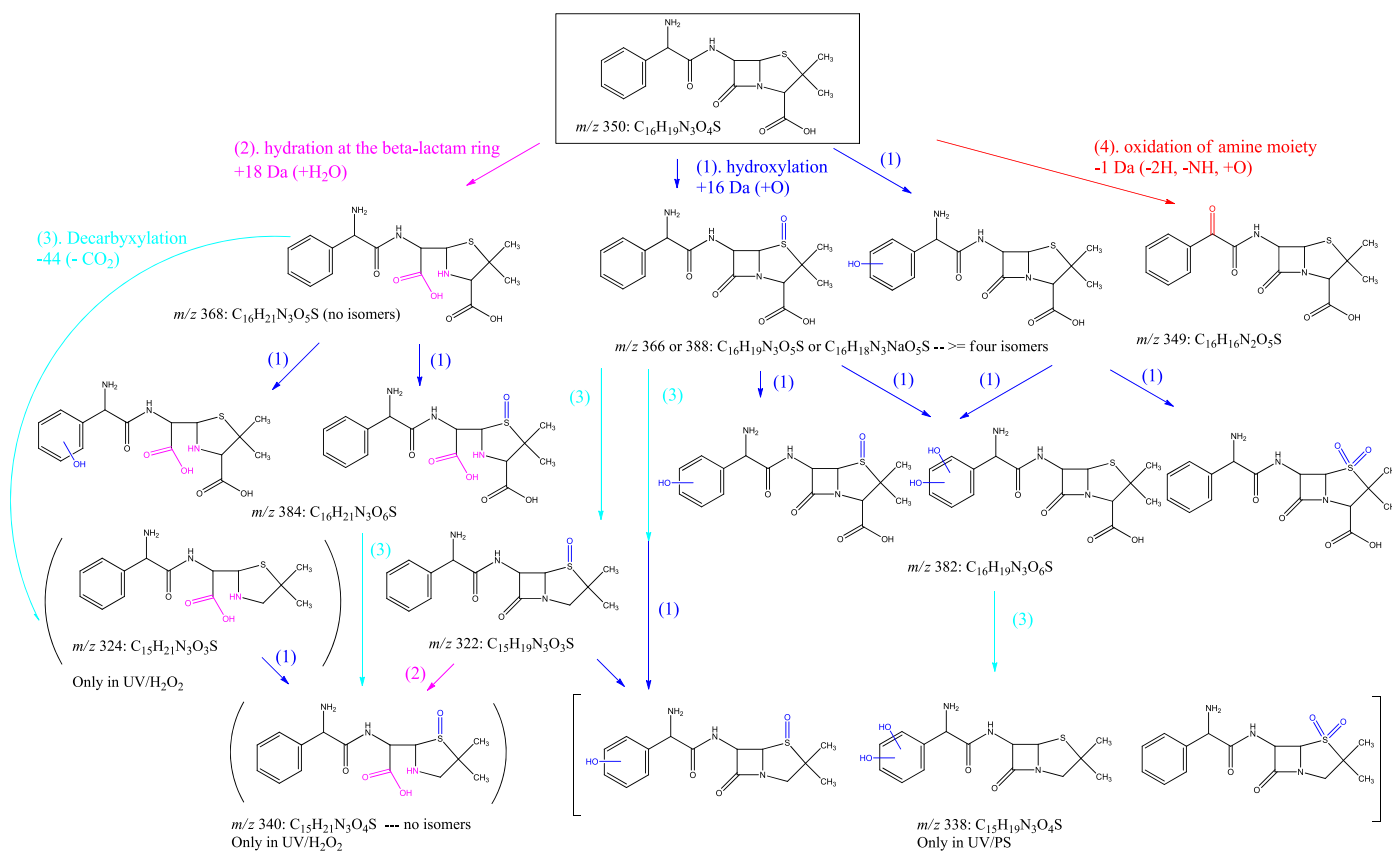
Fig. 5. Possible byproduct formation and pathways of AMP degradation in the UV/H_2O_2 and UV/PS systems, (1) hydroxylation (+16 Da), (2) hydrolysis (+18 Da), (3) decarboxylation (−44 Da) and (4) oxidation of amine into a carbonyl (−1 Da). [Antibiotic]$_0$ = 25 μM; [oxidant]$_0$ = 1 mM.

mass spectrometry analysis, the formation of AMP penilloic acid (i.e., P_{324}, $C_{15}H_{21}N_3O_3S$) from the decarboxylation at the cleaved β-lactam ring of AMP penicilloic acid (i.e., the hydrolysis TP P_{368}) has been reported [55]. With the detection of P_{322} ($C_{15}H_{19}N_3O_3S$, +1O, −CO_2) which was not hydrolysis TPs in this study, the decarboxylation at the five-member ring adjacent to β-lactam ring was also possible as shown in Fig. 5. (4) The hydroxyl group can increase the reactivity of α hydrogen atoms for H-abstraction leading to the formation of a carbonyl [54,57]. The >CH—NH_2 group in AMP could be transformed similarly to an imine >C=NH, with a subsequent carbon-nitrogen double bond cleavage for the formation of a carbonyl >C=O TP P_{349} ($C_{16}H_{16}N_2O_5S$) [58].

As discussed above, in the UV/PS system, both hydroxyl and sulfate radical can be present. The detected TPs in the UV/PS system for the degradation of AMP in this study could thus be from the reactions of both radicals (Fig. 5). In addition, as the hydroxyl radical and sulfate radial can generate the same radical intermediates, it is not surprising to observe similar TPs in the UV/PS and UV/H_2O_2 systems [29,54]. Nevertheless, in the determination of the reaction rate constant of various β-lactam antibiotics with $SO_4^{\bullet-}$ by pulse radiolysis, $SO_4^{\bullet-}$ reacted primarily at the sulfur atom adjacent to the β-lactam ring, resulting in a higher chance of overall antibiotic activity removal [40]. Moreover, the detection of significant abundant P_{338} ($C_{15}H_{19}N_3O_4S$, + 2 O, – CO_2) in UV/PS but not in UV/H_2O_2 might be resulted from the strong electron withdrawing property of $SO_4^{\bullet-}$, i.e., favoring the decarboxylation process [29,54].

3.6.2. PEN, PIP and CEP in the UV/H_2O_2 and UV/PS systems

Both PEN and PIP are penicillin class of antibiotics with a similar five-member ring structure to AMP. Although the analytical limit of our method had led to a much lower variety of TPs detected for these two antibiotics, the major TPs resulted from the proposed mechanisms (1)-(3) in Section 3.6.1 were all observed, i.e., the P_{367} ($C_{16}H_{18}N_2O_6S$, +16 Da), P_{369} ($C_{16}H_{20}N_2O_6S$, +18 Da), and P_{357} ($C_{15}H_{20}N_2O_6S$, or a potassium salt form of P_{395}, $C_{15}H_{19}KN_2O_6S$, +32, +18, and −44 Da) detected in both AOPs for PEN; as well as the P_{534} ($C_{23}H_{27}N_5O_8S$, +16 Da), P_{536} ($C_{23}H_{29}N_5O_8S$, +18 Da), and P_{490} ($C_{22}H_{27}N_5O_6S$, +16 and −44 Da) detected in both AOPs for PIP.

The variety of degradation TPs detected for the six member ring cephalosporin class of antibiotics CEP was even lower for the two data points analyzed. There were no hydrolysis (+18 Da) TPs detected, while the monohydroxylation TPs (P_{435}, $C_{16}H_{15}N_2NaO_7S_2$ or P_{413}, $C_{16}H_{16}N_2O_7S_2$) and decarboxylation TPs (P_{385}, $C_{15}H_{16}N_2O_6S_2$) were detected at a relatively small abundance in this study. The limit of current analytical methods probably contributed to the non-significant detection of the TPs for CEP in the AOPs. More studies such as the MS/MS analysis are needed for a full identification of the TPs formed.

The successful transformation of antibiotics, especially the elimination of the antibiotic active beta-lactam ring, by UV/H_2O_2 and UV/PS may increase the bioavailability of the treated solution which is beneficial for a subsequent activated sludge biological treatment process that is common in wastewater treatment plants after the quenching of oxidant residuals [59]. Though the efficiency of UV/PS appeared to be much higher than UV/H_2O_2, the anaerobic reduction of the sulfate byproduct from persulfate into H_2S may limit its large-scale application [59]. A specific sulfate removal process, such as an extended granular sludge bed reactor, can be considered in this circumstance [59,60]. Under UV irradiation, the presence of a large variety of transition metals in wastewater can improve the degradation efficiency through photo-Fenton or photo-Fenton-like reactions [61]. The application of the mentioned UV-AOPs in treating wastewater, especially those contaminated with transition metals may thus be promising. The photolysis of persulfate using

UV can decrease the pH of reaction solution, which can also lead to an increased degradation of organic pollutants [18]. However, the subsequent pH adjustment may become necessary depending on the requirements of water treatment and quality standard. The treatment efficiencies of UV-based AOPs are strongly influenced by water quality such as turbidity and color as indicated by UV transmittance [59]. As a result, UV-AOPs may be installed after membrane filtration and/or reverse osmosis [62]. In this case, the additional treatment of sulfate anion byproduct and decreased pH need to be considered. Significant energy consumption may also be an inhibition factor for the application of UV-AOPs [59], however, this can be overcome by the integration of recently developed semiconductor light source UV light-emitting diodes (LEDs). UV-LEDs are small device that can be installed freely at various positions of water pipes. In this way, the delivery of UV photons would be more efficient, and the energy efficiency would be much higher than that of conventional UV disinfection or UV water treatment systems. The mercury-free feature and the low voltage source operation system both make UV-LEDs safer to use. The strong energy saving property of UV-LEDs in achieving comparable disinfection purposes will probably make the large-scale UV-LEDs and consequently UV-AOP applications to be promising [63].

4. Conclusions

This study evaluated both kinetics and mechanisms of the degradation of four model β-lactam antibiotics. It was found that direct UV irradiation led to various degrees of photolysis of the antibiotics, correlated to their differences in molar absorptivity at 254 nm. The presence of an oxidant such as persulfate improved significantly the removal efficiency. At a constant UV fluence, different UV fluence rates resulted in the same or comparable degradation of the target compounds. No significant synergistic effect was observed in the presence of both H_2O_2 and $S_2O_8^{2-}$. The presence of common anions such as Cl^-, NO_3^-, and SO_4^{2-} at a 5 mM level did not influence the degradation kinetics either. When nitrobenzene was used as a model compound, the presence of $HO^\bullet$ in the UV/PS system was demonstrated. The steady-state radical concentrations were further estimated revealing a non-negligible contribution of $HO^\bullet$ in the UV/PS system. Contaminant mineralization could also be achieved at high UV fluence, with a slow release of sulfur in the form of SO_4^{2-} and a much slower elimination in TOC levels. The transformation mechanism of the antibiotics in the UV/H_2O_2 and UV/PS systems was investigated showing the main reaction pathways of hydroxylation (+16 Da), hydrolysis (+18 Da) at the β-lactam ring and decarboxylation (−44 Da). This study demonstrates that UV/H_2O_2 and $UV/S_2O_8^{2-}$ AOPs are capable of degrading β-lactam antibiotics and suggests that these processes can potentially decrease the antibiotic activity of the reaction solution.

Acknowledgments

References

[1] J. Davies, D. Davies, Origins and evolution of antibiotic resistance, Microbiol. Mol. Biol. R. 74 (2010) 417–433.

[2] A. Hollis, Z. Ahmed, Preserving antibiotics, rationally, N. Engl. J. Med. 369 (2013) 2474–2476.

[3] E. Meyer, P. Gastmeier, M. Deja, F. Schwab, Antibiotic consumption and resistance: Data from Europe and Germany, Int. J. Med. Microbiol. 303 (2013) 388–395.

[4] FDA, http://www.fda.gov/downloads/ForIndustry/UserFees/AnimalDrugUserFeeActADUFA/UCM338170.pdf (accessed on March 19, 2014). (2011).

[5] R. Hirsch, T. Ternes, K. Haberer, K. Kratz, Occurrence of antibiotics in the aquatic environment, Sci. Total Environ. 225 (1999) 109–118.

[6] D.W. Kolpin, E.T. Furlong, M.T. Meyer, E.M. Thurman, S.D. Zaugg, L.B. Barber, H.T. Buxton, Pharmaceuticals, hormones, and other organic wastewater contaminants in U.S. streams, 1999–2000: a national reconnaissance, Environ. Sci. Technol. 36 (2002) 1202–1211.

[7] K. Kümmerer, Antibiotics in the aquatic environment—a review—Part I, Chemosphere 75 (2009) 417–434.

[8] K. Kümmerer, Antibiotics in the aquatic environment—a review—Part II, Chemosphere 75 (2009) 435–441.

[9] S.K. Khetan, T.J. Collins, Human pharmaceuticals in the aquatic environment: a challenge to green chemistry, Chem. Rev. 107 (2007) 2319–2364.

[10] I. Michael, L. Rizzo, C.S. McArdell, C.M. Manaia, C. Merlin, T. Schwartz, C. Dagot, D. Fatta-Kassinos, Urban wastewater treatment plants as hotspots for the release of antibiotics in the environment: a review, Water Res. 47 (2013) 957–995.

[11] L. Rizzo, C. Manaia, C. Merlin, T. Schwartz, C. Dagot, M.C. Ploy, I. Michael, D. Fatta-Kassinos, Urban wastewater treatment plants as hotspots for antibiotic resistant bacteria and genes spread into the environment: a review, Sci. Total Environ. 447 (2013) 345–360.

[12] I.A. Alaton, S. Dogruel, E. Baykal, G. Gerone, Combined chemical and biological oxidation of penicillin formulation effluent, J. Environ. Manage. 73 (2004) 155–163.

[13] I. Arslan-Alaton, S. Dogruel, Pre-treatment of penicillin formulation effluent by advanced oxidation processes, J. Hazard. Mater. 112 (2004) 105–113.

[14] B.A. Wols, C.H.M. Hofman-Caris, Review of photochemical reaction constants of organic micropollutants required for UV advanced oxidation processes in water, Water Res. 46 (2012) 2815–2827.

[15] A. Tsitonaki, B. Petri, M. Crimi, H. Mosbk, R.L. Siegrist, P.L. Bjerg, In situ chemical oxidation of contaminated soil and groundwater using persulfate: A review, Crit. Rev. Environ. Sci. Technol. 40 (2010) 55–91.

[16] N.S. Shah, X. He, H.M. Khan, J.A. Khan, K.E. O'Shea, D.L. Boccelli, D.D. Dionysiou, Efficient removal of endosulfan from aqueous solution by UV-C/peroxides: A comparative study, J. Hazard. Mater. 263 (2013) 584–592.

[17] X. He, A.A. de la Cruz, D.D. Dionysiou, Destruction of cyanobacterial toxin cylindrospermopsin by hydroxyl radicals and sulfate radicals using UV-254 nm activation of hydrogen peroxide, persulfate and peroxymonosulfate, J. Photochem. Photobiol. A. 251 (2013) 160–166.

[18] J.A. Khan, X. He, H.M. Khan, N.S. Shah, D.D. Dionysiou, Oxidative degradation of atrazine in aqueous solution by $UV/H_2O_2/Fe^{2+}$, $UV/S_2O_8^{2-}/Fe^{2+}$ and $UV/HSO_5^-/Fe^{2+}$ processes: a comparative study, Chem. Eng. J. 218 (2013) 376–383.

[19] X. He, M. Pelaez, J.A. Westrick, K.E. O'Shea, A. Hiskia, T. Triantis, T. Kaloudis, M.I. Stefan, A.A. de la Cruz, D.D. Dionysiou, Efficient removal of microcystin-LR by $UV-C/H_2O_2$ in synthetic and natural water samples, Water Res. 46 (2012) 1501–1510.

[20] O. Legrini, E. Oliveros, A.M. Braun, Photochemical processes for water treatment, Chem. Rev. 93 (1993) 671–698.

[21] R. Qiao, N. Li, X. Qi, Q. Wang, Y. Zhuang, Degradation of microcystin-RR by UV radiation in the presence of hydrogen peroxide, Toxicon 45 (2005) 745–752.

[22] P. Neta, R.E. Huie, A.B. Ross, Rate constants for reactions of inorganic radicals in aqueous solution, J. Phys. Chem. Ref. Data 17 (1988) 1027–1284.

[23] G.V. Buxton, C.L. Greenstock, W. Phillips Helman, A.B. Ross, Critical Review of rate constants for reactions of hydrated electrons, hydrogen atoms and hydroxyl radicals ($^\bullet OH/^\bullet O^-$) in aqueous solution, J. Phys. Chem. Ref. Data 17 (1988) 513–886.

[24] P.M.D. Gara, G.N. Bosio, M.C. Gonzalez, N. Russo, M. Del Carmen Michelini, R.P. Diez, D.O. Mártire, A combined theoretical and experimental study on the oxidation of fulvic acid by the sulfate radical anion, Photochem. Photobiol. Sci. 8 (2009) 992–997.

[25] P. Westerhoff, S.P. Mezyk, W.J. Cooper, D. Minakata, Electron pulse radiolysis determination of hydroxyl radical rate constants with Suwannee River fulvic acid and other dissolved organic matter isolates, Environ. Sci. Technol. 41 (2007) 4640–4646.

[26] G. Mark, M.N. Schuchmann, H. Schuchmann, C. von Sonntag, The photolysis of potassium peroxodisulfate in aqueous solution in the presence of tert-butanol: a simple actinometer for 254 nm radiation, J. Photochem. Photobiol. A 55 (1990) 157–168.

[27] J.H. Baxendale, J.A. Wilson, The photolysis of hydrogen peroxide at high light intensities, Trans. Faraday Soc. 53 (1957) 344–356.

[28] X. He, A.A. de la Cruz, K.E. O'Shea, D.D. Dionysiou, Kinetics and mechanisms of cylindrospermopsin destruction by sulfate radical-based advanced oxidation processes, Water Res. 63 (2014) 168–178.

[29] M.G. Antoniou, A.A. de la Cruz, D.D. Dionysiou, Intermediates and reaction pathways from the degradation of microcystin-LR with sulfate radicals, Environ. Sci. Technol. 44 (2010) 7238–7244.

[30] Wisconsin Department of Natural Resources Laboratory Certification Program, Analytical detection limit guidance & laboratory guide for determining

method detection limits, in: PUBL-TS-056-96, Wisconsin Department of Natural Resources Laboratory Certification Program, 1996.

[31] A.O. Allen, C.J. Hochanadel, J.A. Ghormley, T.W. Davis, Decomposition of water and aqueous solutions under mixed fast neutron and gamma radiation, J. Phys. Chem. 56 (1952) 575–586.

[32] C. Liang, C. Huang, N. Mohanty, R.M. Kurakalva, A rapid spectrophotometric determination of persulfate anion in ISCO, Chemosphere 73 (2008) 1540–1543.

[33] J.R. Bolton, K.G. Linden, Standardization of methods for fluence (UV Dose) determination in bench-scale UV experiments, J. Environ. Eng. 129 (2003) 209–215.

[34] M.I. Stefan, J.R. Bolton, UV direct photolysis of N-nitrosodimethylamine (NDMA): kinetic and product study, Helv. Chim. Acta 85 (2002) 1416–1426.

[35] J.R. Bolton, M.I. Stefan, Fundamental photochemical approach to the concepts of fluence (UV dose) and electrical energy efficiency in photochemical degradation reactions, Res. Chem. Intermediat. 28 (2002) 857–870.

[36] Y. Xiao, R. Fan, L. Zhang, J. Yue, R.D. Webster, T. Lim, Photodegradation of iodinated trihalomethanes in aqueous solution by UV 254 irradiation, Water Res. 49 (2014) 275–285.

[37] E. Hayon, A. Treinin, J. Wilf, Electronic spectra, photochemistry, and autoxidation mechanism of the sulfite-bisulfite-pyrosulfite systems. The $SO_2^{\bullet-}$, $SO_3^{\bullet-}$, $SO_4^{\bullet-}$, and $SO_5^{\bullet-}$ radicals, J. Am. Chem. Soc. 94 (1972) 47–57.

[38] P. Neta, V. Madhavan, H. Zemel, R.W. Fessenden, Rate constants and mechanism of reaction of $SO_4^{\bullet-}$ with aromatic compounds, J. Am. Chem. Soc. 99 (1977) 163–164.

[39] C.L. Clifton, R.E. Huie, Rate constants for hydrogen abstraction reactions of the sulfate radical, $SO_4^{\bullet-}$. Alcohols, Int. J. Chem. Kinet. 21 (1989) 677–687.

[40] K.A. Rickman, S.P. Mezyk, Kinetics and mechanisms of sulfate radical oxidation of ß-lactam antibiotics in water, Chemosphere 81 (2010) 359–365.

[41] J.E. Toth, K.A. Rickman, A.R. Venter, J.J. Kiddle, S.P. Mezyk, Reaction kinetics and efficiencies for the hydroxyl and sulfate radical based oxidation of artificial sweeteners in water, J. Phys. Chem. A 116 (2012) 9819–9824.

[42] S.P. Mezyk, K.A. Rickman, G. McKay, C.M. Hirsch, X. He, D.D. Dionysiou, Remediation of chemically-contaminated waters using sulfate radical reactions: kinetic studies, in: P.G. Tratnyek, T.J. Grundl, S.B. Haderlein (Eds.), ACS Symposium Series 1071: Aquatic Redox Chemistry, Washington, DC, American Chemical Society, 2011, pp. 247–263.

[43] D. Zhao, X. Liao, X. Yan, S.G. Huling, T. Chai, H. Tao, Effect and mechanism of persulfate activated by different methods for PAHs removal in soil, J. Hazard. Mater. 254–255 (2013) 228–235.

[44] V. Nagarajan, R.W. Fessenden, Flash photolysis of transient radicals. 1. X2-with X = Cl, Br, I, and SCN, J. Phys. Chem. 89 (1985) 2330–2335.

[45] X. Yu, Critical evaluation of rate constants and equilibrium constants of hydrogen peroxide photolysis in acidic aqueous solutions containing chloride ions, J. Phys. Chem. Ref. Data 33 (2004) 747–763.

[46] A. Ghauch, A.M. Tuqan, Oxidation of bisoprolol in heated persulfate/H_2O systems: Kinetics and products, Chem. Eng. J. 183 (2012) 162–171.

[47] J.E. Grebel, J.J. Pignatello, W.A. Mitch, Effect of halide ions and carbonates on organic contaminant degradation by hydroxyl radical-based advanced oxidation processes in saline waters, Environ. Sci. Technol. 44 (2010) 6822–6828.

[48] Y. Yang, J.J. Pignatello, J. Ma, W.A. Mitch, Comparison of halide impacts on the efficiency of contaminant degradation by sulfate and hydroxyl radical-based advanced oxidation processes (AOPs), Environ. Sci. Technol. 48 (2014) 2344–2351.

[49] J. Criquet, N.K.V. Leitner, Degradation of acetic acid with sulfate radical generated by persulfate ions photolysis, Chemosphere 77 (2009) 194–200.

[50] J. Kronholm, H. Metsälä, K. Hartonen, M. Riekkola, Oxidation of 4-chloro-3-methylphenol in pressurized hot water/supercritical water with potassium persulfate as oxidant, Environ. Sci. Technol. 35 (2001) 3247–3251.

[51] W. Song, W. Chen, W.J. Cooper, J. Greaves, G.E. Miller, Free-radical destruction of ß-lactam antibiotics in aqueous solution, J. Phys. Chem. A 112 (2008) 7411–7417.

[52] C. Schöneich, K. Bobrowski, Intramolecular hydrogen transfer as the key step in the dissociation of hydroxyl radical adducts of (alkylthio)ethanol derivatives, J. Am. Chem. Soc. 115 (1993) 6538–6547.

[53] A.D. Deshpande, K.G. Baheti, N.R. Chatterjee, Degradation of β-lactam antibiotics, Curr. Sci. 87 (2004) 1684–1695.

[54] X. He, G. Zhang, A.A. de la Cruz, K.E. O'Shea, D.D. Dionysiou, Degradation mechanism of cyanobacterial toxin cylindrospermopsin by hydroxyl radicals in homogeneous UV/H_2O_2 process, Environ. Sci. Technol. 48 (2014) 4495–4504.

[55] A. Ghauch, A. Tuqan, H.A. Assi, Antibiotic removal from water: elimination of amoxicillin and ampicillin by microscale and nanoscale iron particles, Environ. Pollut. 157 (2009) 1626–1635.

[56] W. Zong, F. Sun, X. Sun, Oxidation by-products formation of microcystin-LR exposed to UV/H_2O_2: toward the generative mechanism and biological toxicity, Water Res. 47 (2013) 3211–3219.

[57] S.M. Aschmann, J. Arey, R. Atkinson, Kinetics and products of the reaction of OH radicals with 3-methoxy-3-methyl-1-butanol, Environ. Sci. Technol. 45 (2011) 6896–6901.

[58] E.R. Stadtman, Oxidation of free amino acids and amino acid residues in proteins by radiolysis and by metal-catalyzed reactions, Annu. Rev. Biochem. 62 (1993) 797–821.

[59] J. Dries, A. De Smul, L. Goethals, H. Grootaerd, W. Verstraete, High rate biological treatment of sulfate-rich wastewater in an acetate-fed EGSB reactor, Biodegradation 9 (1998) 103–111.

[60] C. Chen, N. Ren, A. Wang, Z. Yu, D. Lee, Microbial community of granules in expanded granular sludge bed reactor for simultaneous biological removal of sulfate, nitrate and lactate, Appl. Microbiol. Biotechnol. 79 (2008) 1071–1077.

[61] G.P. Anipsitakis, D.D. Dionysiou, Transition metal/UV-based advanced oxidation technologies for water decontamination, Appl. Catal. B: Environ. 54 (2004) 155–163.

[62] C.P. James, E. Germain, S. Judd, Micropollutant removal by advanced oxidation of microfiltered secondary effluent for water reuse, Sep. Purif. Technol. 127 (2014) 77–83.

[63] N. Yeh, P. Yeh, N. Shih, O. Byadgi, T.C. Cheng, Applications of light-emitting diodes in researches conducted in aquatic environment, Renew. Sust. Energ. Rev. 32 (2014) 611–618.